The Plant Cell, Vol. 22: 1564–1574, May 2010, www.plantcell.org © 2010 American Society of Plant Biologists

Conserved Alternative Splicing of *Arabidopsis* Transthyretin-Like Determines Protein Localization and *S*-Allantoin Synthesis in Peroxisomes [C][W]

Ilaria Lamberto,[a] Riccardo Percudani,[a,1] Rita Gatti,[b] Claudia Folli,[a] and Stefania Petrucco[a,2]

[a] Dipartimento di Biochimica e Biologia Molecolare, Università di Parma, 43124 Parma, Italy
[b] Dipartimento di Medicina Sperimentale, Sezione di Istologia, Università di Parma, 43125 Parma, Italy

S-allantoin, a major ureide compound, is produced in plant peroxisomes from oxidized purines. Sequence evidence suggested that the Transthyretin-like (TTL) protein, which interacts with brassinosteroid receptors, may act as a bifunctional enzyme in the synthesis of *S*-allantoin. Here, we show that recombinant TTL from *Arabidopsis thaliana* catalyzes two enzymatic reactions leading to the stereoselective formation of *S*-allantoin, hydrolysis of hydroxyisourate through a C-terminal Urah domain, and decarboxylation of 2-oxo-4-hydroxy-4-carboxy-5-ureidoimidazoline through an N-terminal Urad domain. We found that two different mRNAs are produced from the *TTL* gene through alternative use of two splice acceptor sites. The corresponding proteins differ in the presence (TTL^{1-}) and the absence (TTL^{2-}) of a rare internal peroxisomal targeting signal (PTS2). The two proteins have similar catalytic activity in vitro but different in vivo localization: TTL^{1-} localizes in peroxisomes, whereas TTL^{2-} localizes in the cytosol. Similar splice variants are present in monocots and dicots. TTL originated in green algae through a Urad-Urah fusion, which entrapped an N-terminal PTS2 between the two domains. The presence of this gene in all Viridiplantae indicates that *S*-allantoin biosynthesis has general significance in plant nitrogen metabolism, while conservation of alternative splicing suggests that this mechanism has general implications in the regulation of the ureide pathway in flowering plants.

INTRODUCTION

Plants depend on efficient nitrogen uptake and nitrogen redistribution to sustain their growth. Following assimilation or fixation, nitrogen is transported from the root to the aerial portions of the plant in the form of amino acids or ureides, primarily allantoin and allantoate (Schubert, 1986). Amino acids and ureides thus act as major nitrogen transport compounds as well as nitrogen storage forms within plant cells. In fact, there is no excretion of waste nitrogen in plants.

Allantoin and its hydrolysis product, allantoic acid, are nitrogen-rich compounds with a high N:C ratio (1:1) derived from the degradation of purines. Although the metabolism of these compounds has been particularly investigated in tropical legumes (where ureides can account for up to 95% of the nitrogen present in the xylem sap), some evidence indicates that the ability to recover nitrogen from purines originated in green algae and is a general feature of plants (Todd et al., 2006). A first step of purine catabolism occurs in the cytoplasm and leads to the production of oxopurines, such as hypoxanthine, xanthine, and uric acid. Uric acid is then transferred into the peroxisome and further metabolized to allantoin; hydrolysis of allantoin in the endoplasmic reticulum yields allantoic acid (Hanks et al., 1981). Depending on growth requirements, ureides can accumulate or be further metabolized in the endoplasmic reticulum (Werner et al., 2008), making the nitrogen stored in the purine bases accessible for subsequent anabolic reactions.

Until recently, the enzymatic activities required for the stereoselective conversion of uric acid into *S*-allantoin (Figure 1) were unknown. The true product of the urate oxidase (Uox) reaction is 5-hydroxyisourate (HIU), and its hydrolysis yields 2-oxo-4-hydroxy-4-carboxy-5-ureidoimidazoline (OHCU), an intermediate in the formation of allantoin (Kahn and Tipton, 1998). A gene encoding a protein with HIU hydrolase (HIUase) activity related by homology to glucosidases has been described in soybean (*Glycine max*) root nodules (Raychaudhuri and Tipton, 2002), whereas a different HIUase, related to transthyretin, is encoded by bacterial (*pucM*) and mammalian (*urah*) genes. Finally, a gene coding for OHCU decarboxylase (*urad*) has been found to be required for the stereoselective formation of *S*-allantoin (Ramazzina et al., 2006). Remarkably, it has been shown that the thyroid hormone transporter transthyretin originated in vertebrates by duplication of the *urah* gene (Zanotti et al., 2006). Such a finding implies that very different roles, such as enzymatic activities and hormone transport, can be accomplished by proteins containing the HIUase fold.

The *Arabidopsis thaliana* transthyretin-like gene (*TTL*) encodes a putative bifunctional protein with sequence similarity to both Urah and Urad domains (Ramazzina et al., 2006). Interestingly,

[1] Address correspondence to riccardo.percudani@unipr.it.
[2] Stefania Petrucco passed away on February 23, 2009.
The author responsible for distribution of materials integral to the findings presented in this article in accordance with the policy described in the Instructions for Authors (www.plantcell.org) is: Riccardo Percudani (riccardo.percudani@unipr.it).
[C] Some figures in this article are displayed in color online but in black and white in the print edition.
[W] Online version contains Web-only data.
www.plantcell.org/cgi/doi/10.1105/tpc.109.070102

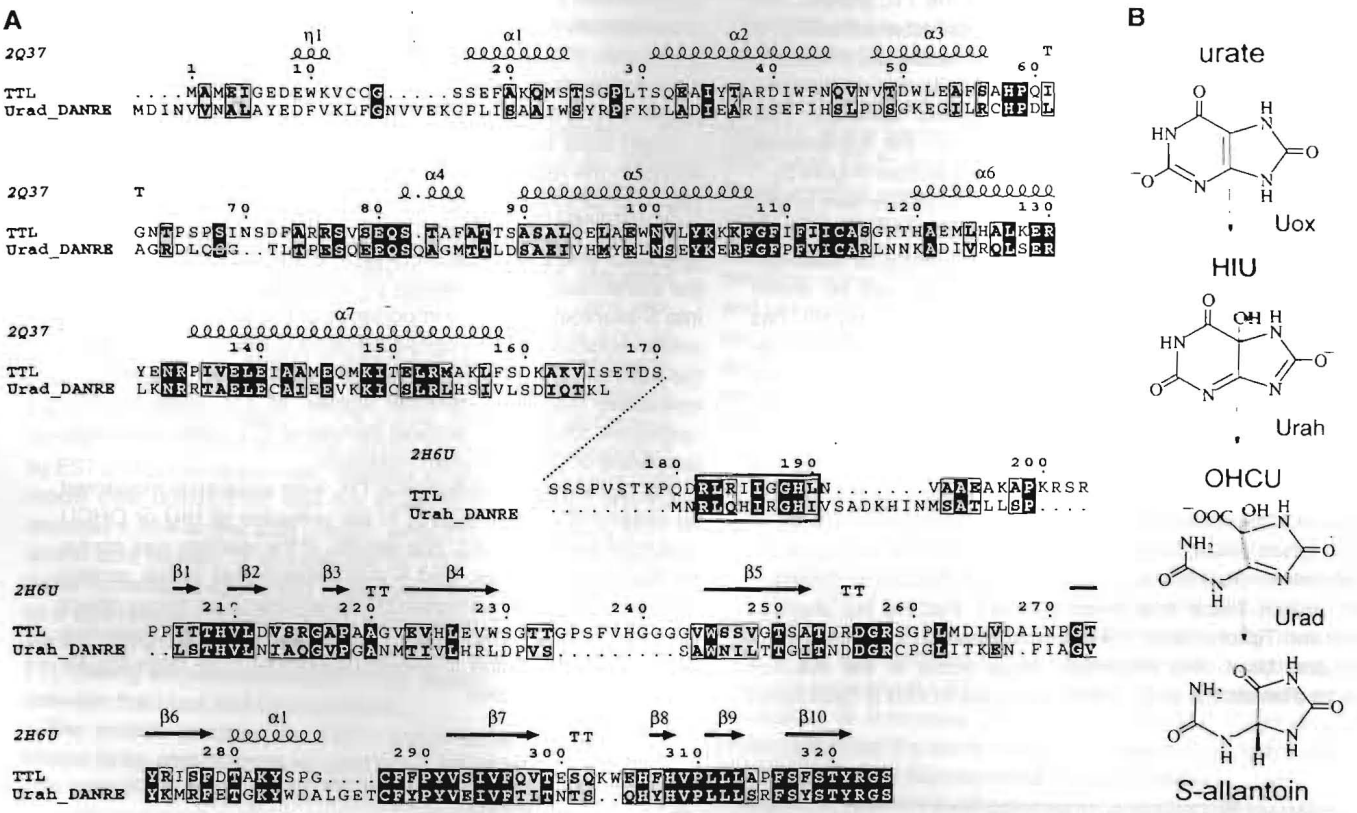

Figure 1. Sequence Comparison Suggests a Role for TTL in Allantoin Biosynthesis.

(A) Alignment of TTL with Urad and Urah protein from zebrafish. Conserved positions are shaded according with the Espript (Gouet et al., 1999) similarity criteria. The sequence motif corresponding to the PTS2 consensus is boxed. Secondary structure elements derived from the three-dimensional coordinates of the Urad domain from *Arabidopsis* (Kim et al., 2007) and the Urah domain from zebrafish (Zanotti et al., 2006) are drawn above the alignment.

(B) Scheme of the enzymatic pathway for the formation of *S*-allantoin from uric acid.

[See online article for color version of this figure.]

biochemical and genetic studies have provided evidence that this protein is a potential substrate of the brassinosteroid receptor kinase at the plasma membrane, and it has been hypothesized that in *Arabidopsis*, TTL behaves as a negative regulator in brassinosteroid-mediated plant growth (Nam and Li, 2004). On the other hand, the TTL protein contains a sequence resembling a peroxisome targeting signal (Hennebry et al., 2006), and it has been found as a component of *Arabidopsis* leaf peroxisomes (Reumann et al., 2007). Moreover, structural studies have shown that the Urad domain of TTL binds *S*-allantoin and has structural similarity to vertebrate OHCU decarboxylase (Kim et al., 2007). Altogether, these observations suggest that the *Arabidopsis* TTL protein plays a dual role in plant growth, both in modulating brassinosteroid hormone responses and ureide synthesis.

We thus decided to characterize the enzymatic properties and the intracellular localization of the *Arabidopsis* TTL protein. We found that two alternative splice variants of the TTL protein are present in *Arabidopsis*, one being localized in the peroxisomes and the other in the cytosol. However, both protein variants exhibit *S*-allantoin synthase activity in vitro. Alternative splicing is conserved in flowering plants, and the relative amount of the two spliced transcripts appears to vary in different tissues and growth conditions. We propose that modulation of the relative amounts of the peroxisomal versus cytosolic TTL by alternative splicing affects ureide biosynthesis in plant cells.

RESULTS

TTL Encodes a Bifunctional HIU Hydrolase-OHCU Decarboxylase (*S*-Allantoin Synthase)

Comparison of the amino acid sequence of *Arabidopsis* TTL with Urad and Urah proteins from zebrafish shows that TTL is a bidomain protein containing a Urad domain at the N terminus and a Urah domain at the C terminus (Figure 1A). The two domains are separated by a linker of 24 amino acids, which includes a type 2 peroxisome target sequence (PTS2; RLx_5HL), which is consistent with the notion that allantoin biosynthesis occurs in the peroxisomes.

To evaluate its properties as a bifunctional enzyme in the pathway leading to the synthesis of *S*-allantoin (Figure 1B), we

decided to clone, overexpress, and purify the TTL protein. The full-length coding sequence of TTL was amplified and the 972-bp PCR product was cloned in a bacterial vector for the overexpression of His-tagged TTL. Following affinity chromatography (see Supplemental Figure 1 online), purified full-length His-tagged TTL enzyme activity was tested on the compounds involved in the conversion of uric acid into allantoin (Figure 2).

Because the intermediates involved in the conversion of uric acid into allantoin are optically active compounds, the reactions can be followed by observing circular dichroism (CD) spectroscopy. The two intermediates, HIU and OHCU, can be distinguished by observing CD signals at 312 nm, where only HIU has appreciable ellipticity, and at 257 nm, where only OHCU has appreciable ellipticity (Figure 2A). When only urate oxidase and uric acid are present in the reaction mixture, levorotatory HIU is initially produced (Figure 1B, step 1), as revealed by the formation of a negative peak around 312 nm. Spontaneous hydrolysis of HIU then produces levorotatory OHCU, as revealed by formation of a negative peak around 257 nm. Spontaneous decay of OHCU gives allantoin as a stable end product. At millimolar substrate concentrations, the urate oxidase reaction is complete after several hours and yields optically inactive RS-allantoin (Kahn and Tipton, 1998). On the other hand, in the presence of Urah and Urad, two enzymatic steps occur in the reaction mixture (Ramazzina et al., 2006): levorotatory HIU is hydrolyzed to levorotatory OHCU by Urah (Figure 1B, step 2), and OHCU is stereoselectively decarboxylated by Urad to give dextrotatory *S*-allantoin (Figure 1B, step 3). Accumulation of *S*-allantoin in the reaction mixture can be monitored due to its characteristic peaks around 220 and 242 nm (Figure 2A).

When urate oxidase and purified *Arabidopsis* TTL were both added in the reaction mixture, we observed the rapid decay of HIU and OHCU, and formation of optically active *S*-allantoin (Figure 2B). This result proves that TTL encodes a protein with HIU hydrolase and OHCU decarboxylase activities, able to catalyze the stereoselective conversion of uric acid oxydation products into *S*-allantoin. Given the importance of this latter compound in ureide metabolism, we propose the name *S*-allantoin synthase for the plant enzyme. Based on sequence comparison (Figure 1), we concluded that the C-terminal domain of TTL catalyzes HIU hydrolysis, while the N-terminal domain of TTL catalyzes decarboxylation of OHCU to give *S*-allantoin.

The two enzymatic activities of TTL were separately monitored by observing enzyme activity in the presence of HIU or OHCU as substrates (Figure 2C). The velocity of the reaction was similar for the two substrates, and it was proportional to the protein concentration. After correction for the spontaneous decay rate of the substrates, we calculated a specific activity of ~30 units/mg for HIU hydrolysis and a specific activity of ~26 units/mg for OHCU decarboxylation.

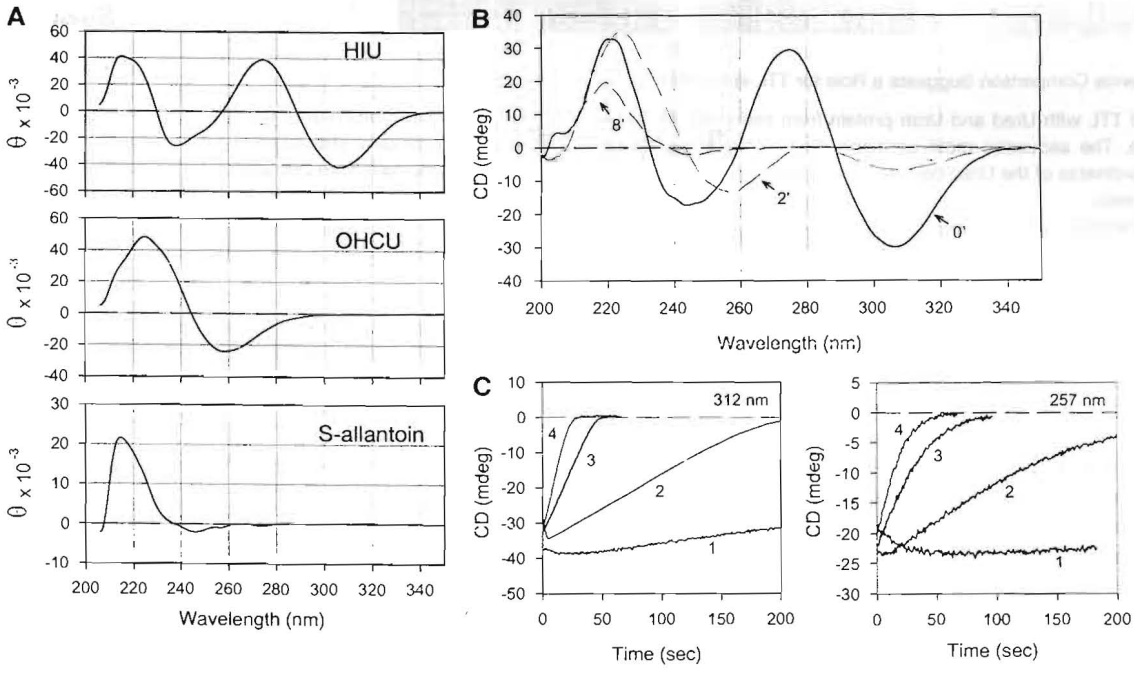

Figure 2. Biochemical Activity of TTL as *S*-Allantoin Synthase.

(A) Approximate CD spectra of the chiral molecules involved in ureide biosynthesis (θ, molar ellipticity).

(B) Time-resolved CD spectra of the conversion of uric acid (0.1 mM in 100 mM potassium phosphate, pH 7.6) in the presence of urate oxidase and *Arabidopsis* TTL (10 nM).

(C) Conversion of HIU (left panel; 312 nm) and OCHU (right panel; 257 nm) substrates in the presence of different TTL concentrations: (1) no enzyme, (2) 10 nM, (3) 100 nM, and (4) 200 nM. Substrates were generated immediately before the reaction using uric acid (0.1 mM in 100 mM potassium phosphate, pH 7.6) and urate oxidase (for HIU) or urate oxidase plus zebrafish HIU hydrolase (for OHCU).

Two TTL Variants Differing by the Presence of an Internal Peroxisomal Targeting Signal Are Produced by Alternative Splicing

Analysis of database sequences suggests the presence of alternative splice forms of the *TTL* gene (Hennebry et al., 2006; Reumann et al., 2007). We used RT-PCR of total RNA extracted from *Arabidopsis* seedlings to amplify transcription products of *TTL*. Gel electrophoresis indicated the presence of two different species in the amplification products. Cloning and sequence analyses revealed that alternative splicing of the *TTL* gene produces two transcript forms (Figure 3), designated in this work as TTL^{1-} and TTL^{2-} according to a recent proposed nomenclature (Sammeth et al., 2008). These splicing variants correspond to transcript models present in the public databases (accession numbers NM_125207 and NM_001037017) and are supported by EST and cDNA sequences, whereas a third putative transcript model (NM_001037016) was not found in our analysis. TTL^{1-} encodes a 324–amino acid protein, while TTL^{2-} encodes a 311–amino acid protein. In comparison to TTL^{1-}, the TTL^{2-} mRNA lacks nucleotides 883 to 921 of the pre-mRNA due to the usage of a downstream splice acceptor site within the third intron of the *TTL* gene (Figure 3B). Interestingly, the missing portion of the TTL coding sequence contains PTS2, located within the linker between the Urad and Urah domains.

The protein encoded by TTL^{1-} splice variant was already shown to be able to catalyze synthesis of *S*-allantoin (Figure 2). The protein encoded by the TTL^{2-} variant was produced in a recombinant form using a similar procedure and assayed for activity in the same reaction conditions. This protein was found to be active, with specific activities for HIU hydrolysis and OHCU decarboxylation comparable to those measured for TTL^{1-}.

TTL Splice Variants Have Different Intracellular Localizations

To clarify the subcellular localization of the two previously identified TTL splice variants, we constructed C-terminal fusions of TTL^{1-} and TTL^{2-} with the green fluorescent protein (GFP). The fusion proteins were transiently expressed in *Arabidopsis* protoplasts and coexpressed with markers for peroxisome or cytoplasm. A yellow fluorescent protein with a C-terminal Ser-Lys-Leu targeting signal (YFP-SKL) was used as a peroxisomal marker, and unmodified YFP was used as a cytosolic marker. Unlabeled samples were used to establish the levels and locations of the autofluorescence due to plastids, and single-labeled controls were used to assess bleed-through between fluorochromes. These procedures allowed selection of emission filter sets giving negligible crosstalk between fluorochromes in the different detection channels.

Upon transient expression, TTL^{1-}-GFP localized to punctate cellular structures overlapping with the structures labeled by the peroxisomal YFP, whereas TTL^{2-}-GFP colocalized with the cytosolic YFP (Figure 4). Given the unusual internal position of the PTS2 signal of TTL^{1-}, to rule out the possibility that the TTL^{1-}-GFP was directed to the peroxisome after a proteolytic cleavage exposing the PTS2 at the N terminus, we observed the localization of N-terminal GFP fusions. The GFP-TTL^{1-} fusion protein exhibited the same punctate localization as TTL^{1-}-GFP and YSP-SKL (see Supplemental Figure 2 online).

We concluded from these colocalization studies that the internal PTS2 signal of TTL^{1-} can direct the bifunctional *S*-allantoin synthase to the site where ureide synthesis occurs, namely, peroxisomes. In the absence of the differentially spliced targeting signal, TTL^{2-} is incapable of entering the peroxisomes, and the

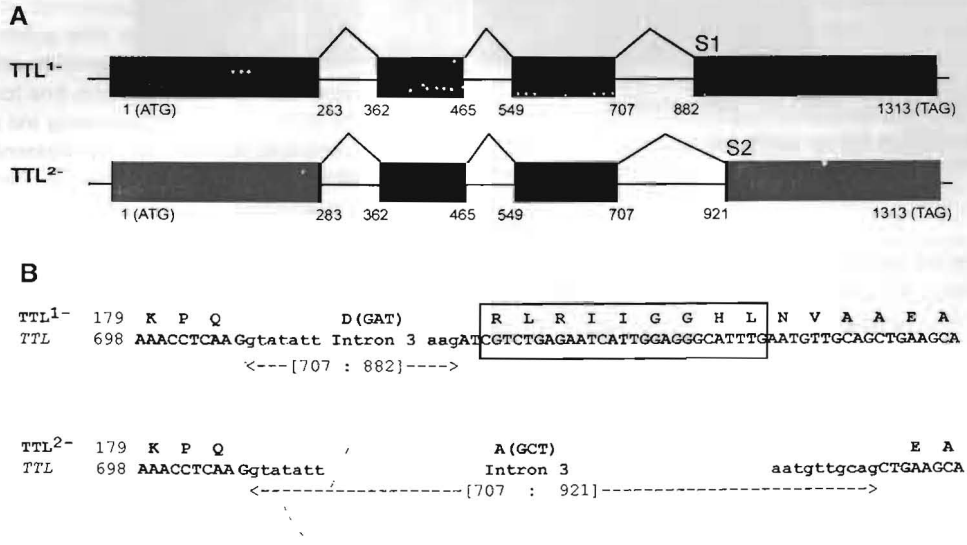

Figure 3. Alternative Splicing in TTL.

(A) Schematic overview of the transcript variants of the *Arabidopsis TTL* gene. The intron boundaries are numbered.

(B) Sequence detail of the alternative splicing as deduced by Genewise comparison of the transcript variants with the *TTL* gene; transcript variants are written as amino acid sequences, codons comprised in exons are written in uppercase letters below the corresponding amino acid, and intronic sequences are written in lowercase letters. The sequence corresponding to the PTS2 consensus is boxed.

[See online article for color version of this figure.]

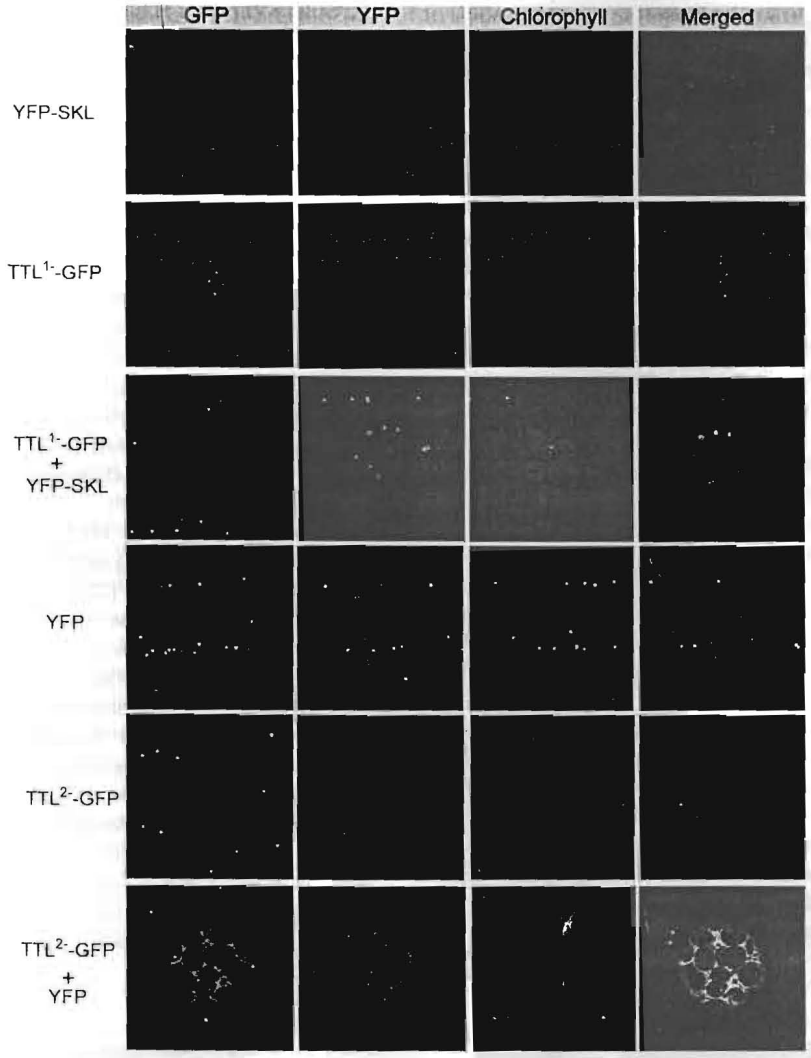

Figure 4. In Vivo Localization of TTL^{1-} and TTL^{2-} Splice Variants.

Fluorescence in the range of 490 to 510 nm (GFP), 542 to 596 nm (YFP), and 649 to 767 nm (chlorophylls) was monitored in transformed *Arabidopsis* protoplasts using confocal microscopy. Detection channels and three-channel merged images are indicated by column labels. Transformants are indicated by row labels.

protein is thus retained in the cytosol. From our studies, we could not detect any differences in cytosolic YFP and TTL^{2-}-fused GFP, suggesting that the previously observed membrane association (Nam and Li, 2004) could not be detected in our transient expression system.

Evolutionary Conservation of TTL Alternative Splicing in Flowering Plants

Analysis of EST sequences suggests that alternative splicing of the internal PTS2 sequence of TTL may also occur in other plants (Hennebry et al., 2006; Reumann et al., 2007). Conservation of alternatively spliced forms in evolutionarily distant species is further evidence that this mechanism may play a biologically significant role. To validate the occurrence of a similar mechanism in distant plant species, we investigated by RT-PCR the existence of differently spliced transcripts in *Oryza sativa*. PCR primers were designed to amplify the linker region between the Urad and Urah domains. Gel electrophoresis of the amplification product showed the existence of two transcripts differing by about 50 nucleotides, similar to what is observed in *Arabidopsis* (Figure 5). Sequencing of the cloned PCR products and comparison with the *TTL* gene sequence (see Supplemental Figure 3 online) revealed that in *O. sativa*, two transcripts are produced through alternative splicing. As in *Arabidopsis*, the intron undergoing alternative splicing is a phase 1 intron located between the two domains, and the splice donor and the first splice acceptor site (S1) occupy the same position in the two organisms. The alternative acceptor site (S2) is located 39 nucleotides downstream in *Arabidopsis* and 60 nucleotides downstream in *O. sativa*.

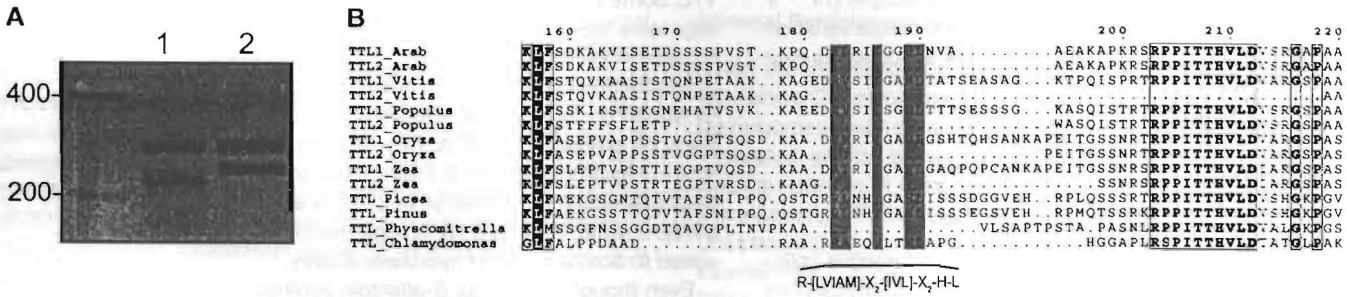

Figure 5. Conservation of TTL Alternative Splicing in Plants.

(A) RT-PCR analysis of TTL splice variants in *O. sativa* (line 1) and *Arabidopsis* (line 2). Total RNA was extracted from whole plants, and PCR products were fractionated on an ethidium bromide–stained agarose gel.

(B) Alignment of the linker region between Urad and Urah domains in various plants. Sequences were retrieved by homology searches in protein and EST databases (accession numbers are reported in Supplemental Table 1 online) and aligned with ClustalW. Conserved positions are shaded according with Espript (Gouet et al., 1999). The sequence motif corresponding to the PTS2 consensus is indicated.

[See online article for color version of this figure.]

Having found experimental confirmation of TTL splice variants deduced by EST analysis, we looked for additional examples of alternative splicing by analyzing protein alignment of TTL orthologs retrieved through similarity searches in The Institute for Genomic Research (TIGR) plant transcript assemblies database (see Methods). In this analysis, we found evidence of splice forms differing by the presence or the absence of the internal PTS2 in various plant species (Figure 5B). In many cases, comparison with available genomic sequences made it possible to identify alternative splice sites. A single TTL variant derives from intronless genes in the green alga *Chlamydomonas reinhardtii* and the moss *Physcomitrella patens*, with a recognizable PTS2 present in *C. reinhardtii* but not in *P. patens*. No evidence for alternative splicing was found in Gymonospermae, which were found always to encode proteins with an internal PTS2. By contrast, evidence of alternative splicing is present in several Angiospermae, both in monocot and dicot species. In most cases examined, splice variants are generated by the use of an alternative splice acceptor site located between the Urad and Urah domain, resulting in the inclusion or exclusion of the internal PTS2 in the coding sequence and leaving the catalytic domains intact.

Expression of TTL Splice Forms in *Arabidopsis*

To obtain insights on the expression of the TTL splice variants, the presence of TTL^{1-} and TTL^{2-} transcripts in the whole *Arabidopsis* plant and in different tissues was assessed by means of RT-PCR (Figure 6). Both splicing variants were detected in the samples analyzed, and the relative proportion of the TTL^{1-} and TTL^{2-} forms did vary in the different organs tested (Figure 6). A similar proportion of TTL^{1-} and TTL^{2-} transcripts was usually observed in the different tissues analyzed, with the exception of floral buds, which appear to accumulate a higher proportion of the cytosolic form (TTL^{2-}).

On the basis of the role of *S*-allantoin synthase in ureide biosynthesis, we also compared mRNA levels in plantlets grown on uric acid or allantoin as nitrogen sources (see Supplemental Figure 4 online). With uric acid (5 mM) as the sole nitrogen source, the seed germinated, but seedlings did not develop; to obtain growth beyond the cotyledon stage, low nitrogen (5 mM NH_4NO_3) had to be included in the growth media. In the presence of 5 mM allantoin, seedlings exhibited a phenotype with small, green leaves and strong root elongation as already reported (Desimone et al., 2002). The expectation was that higher levels of TTL^{1-} would be required for the cell to use the nitrogen stored in uric acid, while lower levels of TTL^{1-} were expected in the presence of allantoin, the product of the reaction catalyzed by the enzyme. However, in these experiments, we did not find a substantial variation in the level of the two splice forms, suggesting that the presence of exogenous ureides in the growth media does not affect expression of the gene in *Arabidopsis*. It has recently been reported that ureides accumulate in *Arabidopsis* plants exposed to darkness and that TTL is among the genes induced during dark stress (Brychkova et al., 2008). The amount of TTL^{1-} and TTL^{2-} transcripts in plants placed in the dark for 2, 4, and 6 d was analyzed and compared with SRG1 mRNA, a well known dark-induced transcript. In our experiments, we did not

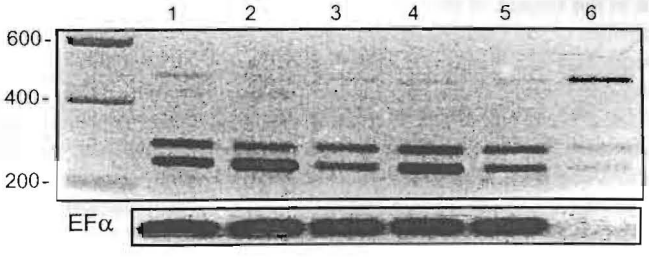

Figure 6. RT-PCR Analysis of TTL Splice Variants in Different *Arabidopsis* Tissues.

PCR products were fractionated on an ethidium bromide–stained agarose gel. Total RNA was extracted from plant stem (lane 1), floral buds (lane 2), flower (lane 3), rosette leaves (lane 4), and 3-d-old seedlings (lane 5). The control PCR reaction was conducted in the absence of reverse transcriptase (lane 6). Elongation Factor 1-α (EFα) was used as a reference gene.

observe an increase of the total level of TTL transcripts (TTL^{1-} + TTL^{2}) in plants exposed to darkness nor a noticeable variation of the relative proportion of the two alternative splice forms (see Supplemental Figure 5 online).

DISCUSSION

TTL Function and Regulation

Two distinct proteins are produced through the alternative splicing of the TTL pre-mRNA. One splice variant (TTL^{1-}) contains an internal PTS2 sequence and enters into *Arabidopsis* peroxisomes. Peroxisomal localization of both C-terminal and N-terminal GFP fusions indicates that insertion into peroxisomes does not require N-terminal processing of the protein. PTS2 sequences are usually cleaved upon peroxisomal import by a specific protease (Helm et al., 2007); in this case, cleavage would separate the catalytic domains of the protein into two separate chains. Cleavage of TTL to form the typical transthyretin tetramer has been previously supposed (Hennebry et al., 2006). There is evidence that this process does not take place in TTL. The protein lacks a conserved Cys residue downstream from the PTS2 that is required for the cleavage, and bidimensional electrophoresis indicates the presence of the whole TTL protein in plant peroxisomes (Reumann et al., 2007; Eubel et al., 2008). Consistent with these observations, we demonstrated that the whole protein is able to catalyze two consecutive reactions that lead to *S*-allantoin synthesis.

The presence of two enzymatic domains in a single chain could provide a catalytic advantage if the product of one enzyme were transferred directly to the other enzyme without being released in solution. This mechanism, known as substrate channeling (Miles et al., 1999), could be particularly useful for protecting a labile intermediate (OHCU in this case) from solvent. Our data, however, do not provide support for the existence of channeling in TTL. When tested with the two substrates in solution, activity toward OHCU appeared to be only slightly lower than activity toward HIU (Figure 2C). If an efficient mechanism of channeling is in place, one should not expect to see accumulation of OHCU in solution when HIU is used as substrate for the protein. Contrary to this expectation, the OHCU intermediate appeared to accumulate in the course of the reaction (Figure 2B). We compared the activities of the bifunctional enzyme with the activities of the two separated enzymes from zebrafish measured in the same reaction conditions. Interestingly, zebrafish OHCU decarboxylase has a similar activity (~53 units/mg), whereas the activity of HIU hydrolase is one order of magnitude higher (~500 units/mg). This could suggest the existence in the bifunctional enzyme of allosteric interactions that synchronize the reactions and prevent the buildup of excess intermediates.

A second splice variant of TTL (TTL^{2-}) does not contain the internal PTS2 sequence and is localized in the cytosol. This protein was found to be catalytically active in vitro. Although alternative splicing apparently does not alter the catalytic domains (cf. Figures 1 and 3), this result is not trivial because a modification of the linker region between the two domains could easily alter the oligomeric organization of the protein. We tried various techniques to obtain direct evidence of the oligomeric organization of TTL. Some indications of a heterogeneous composition of protein oligomers were obtained by atomic force microscopy and gel filtration (data not shown), but the protein's tendency to aggregate in concentrated solutions prevented an accurate assessment of its quaternary organization. However, it is known from the structures of prokaryotic and eukaryotic HIU hydrolases that two active sites are formed at the interface between the two dimers that build up the protein tetramer (Jung et al., 2006; Zanotti et al., 2006). Therefore, a tetrameric organization of TTL must be invoked to account for HIU hydrolase activity.

Even though TTL^{2-} has *S*-allantoin synthase activity in vitro, this could hardly be the function of the protein in vivo. HIU is an unstable substrate that should be only produced in peroxisomes through oxidation of urate by urate oxidase, a prototypical peroxisomal enzyme in eukaryotes. The cytosolic localization of the TTL^{2-} splice variant thus suggests a different function for the protein. These observations could reconcile data presented here, indicating a role in the ureide pathway, with previous evidence suggesting a role in hormone signaling (Nam and Li, 2004). Although we did not observe plasma membrane localization of the GFP fusion protein in our system, presence of the protein in the cytosol would be compatible with the supposed interaction with a plasma membrane brassinosteroid receptor. Expression data showed that the relative proportion of the two splice forms of TTL vary in different plant tissue and growth conditions. Given that data on enzymatic activity indicate that the protein chains can associate in oligomeric structures regardless of the presence of a PTS2 in the linker region, it is likely that localization and function of peptide chains produced by a splice variant are affected by the presence of peptide chains produced by the other splice variant. Such interaction among splice variants opens the possibility for subtle mechanisms of regulation at the posttranscriptional and posttranslational level.

Significance and Conservation of TTL Alternative Splicing

Production of splice variants in TTL depends on the use of alternative 3′ acceptor sites. After exon retention, this is the second most common mechanism of alternative splicing both in plants and humans (Wang and Brendel, 2006; Sammeth et al., 2008). A peculiar feature of the TTL alternative splicing is the involvement of an internal peroxisomal targeting signal. In general, the majority of subcellular localization signals, including signals for the endoplasmic reticulum, mitochondria, and chloroplast, are located near the protein N terminus. Thus, the production of mRNAs encoding proteins with different cellular localization often depends on the use of alternative transcription start sites rather than alternative splicing (Prassinos et al., 2008; Puyaubert et al., 2008). However, examples exist in plants of alternative splicing involving subcellular localization signals. Two splice variants of protein Ser/Thr phosphatase 5 (PP5), a protein involved in signal transduction, are produced in *Solanum lycopersicum*, with a shorter PP5 isoform localized in both the nucleus and the cytoplasm and a larger isoform targeted to the endoplasmic reticulum (de la Fuente van Bentem et al., 2003). In *Arabidopsis*, two proteins belonging to the glutathione *S*-transferase (GST) superfamily form fusions with Myb transcription factor-like domains through alternative splicing;

addition of this domain at the C terminus masks a peroxisomal targeting signal and redirects the proteins to the nucleus (Dixon et al., 2009). Pumpkin (*Cucurbita* sp cv Kurokawa Amakuri Nankin) hydroxypyruvate reductase is produced by alternative splicing with and without a C-terminal signal for targeting to peroxisomes (Hayashi et al., 1996). These and other examples demonstrate alternative splicing events involving the C-terminal PTS1 sequence, and this work shows TTL to be an example of dual subcellular localization involving alternative splicing of a PTS2 sequence.

Alternative splicing is considered a mechanism for increasing the functional repertoire of the plant proteome (Kazan, 2003; Wang and Brendel, 2006; Reddy, 2007; Barbazuk et al., 2008). Interestingly, we observed conservation of TTL alternative splicing in flowering plants, organisms that have more splice regulators than other eukaryotes. Although alternative splicing is commonly observed in flowering plants, conservation of splicing in different species is observed more rarely and is generally considered an indication that splice variants have specific functional roles.

Origin of the *urad-urah* Gene Fusion in Plants

In metazoa, fungi, and most bacteria, the Urad and Urah domain are encoded by separated genes, whereas in plants and some bacteria, the two catalytic domains are fused in a single gene. The C-terminal part of Urah (particularly the tetrapeptide YRGS) is universally conserved in the protein, and the analysis of the active site indicates a functional role for the free carboxylate group in C-terminal position (Jung et al., 2006; Zanotti et al., 2006). This suggests that the gene fusion between the two domains can encode a functional protein only if Urah is at the C terminus. In keeping with these considerations, in bacteria the domain order is Urad-Urah, the same as in plants. Surprisingly, however, the bifunctional bacterial genes are not among the first prokaryotic hits found by homology searches using the plant protein as a query.

Phylogenetic trees of the Urad and Urah domains suggest an independent origin for the bacterial and plant gene fusions (see Supplemental Figure 6 and Supplemental Data Sets 1 and 2 online), with the plant proteins being more related to proteins that are encoded by separated genes in marine γ-proteobacteria such as *Halella* and *Congregibacter*. Interestingly, the two domains appear to be encoded by separated genes also in the green alga *Micromonas*: Urad is encoded on chromosome 4 and contains a PTS1 C-terminal sequence (AKL-COOH), while Urah is encoded on chromosome 5 and apparently does not contain peroxisome targeting signals. The domain fusion, however, is present in the green alga *C. reinhardtii*, in which an intronless gene encodes a bidomain protein with an internal PTS2 signal (Figure 5). *Micromonas* belongs to Prasinophytae, a taxonomic group believed to retain characteristics of the ancestors of chlorophytes (green algae) and streptophytes (land plants and charophyte algae) (Worden et al., 2009). The data presented here suggest that the Urad-Urah fusion occurred in a green alga ancestor before the split of chlorophytes and streptophytes but possibly after the divergence of Prasinophytae. Since TTL genes were probably present at the origin of Viridiplantae, the *urad-urah* gene fusion could be a useful phylogenetic marker to study the deepest branches of green algae evolution.

Internal Peroxisome Targeting Signals Are Rare

Given the incompatibility between the catalytic C terminus of Urah and a C-terminal targeting signal, targeting of this protein to peroxisomes involves a different pathway. When encoded by separated genes, eukaryotic Urah proteins have a PTS2 sequence near the N terminus, whereas Urad proteins have the more common PTS1 sequence. Fusion between an N-terminal Urad and a C-terminal Urah naturally eliminated PTS1 and left an internal PTS2. In general, a fusion between two domains with PTS1 and PTS2 sequences will create a protein with an internal targeting signal if the order of the gene fusion is the same as in TTL or a protein with a double targeting signal at conventional positions (N-terminal PTS2, C-terminal PTS1) if the gene fusion is in the opposite order. Besides TTL, the only other case of internal PTS2 has been described in the fungus *Penicillium chrysogenum* (Kiel et al., 2009). As for TTL, it is a fusion protein that contains an internal PTS2 between two functional domains (fumarate reductase and cytochrome b5).

Given that only a fraction of the gene fusion events between peroxisomal proteins can result in internal PTSs, the occurrence of this type of signals is expected to be rare. To seek other cases of internal PTS2, we searched the proteome of *Arabidopsis* for the occurrence of a nonapeptide motif built from the alignment of TTL targeting signals (Figure 5). The resulting pattern (R-[LVMIA]-X-X-[ILV]-X-X-H-L) occurs 122 times in the *Arabidopsis* proteome; 25 times near the N terminus (position <50) and 87 times far from the N terminus (position >100). Many of these latter cases apparently are chance occurrences of the motif in non-peroxisomal proteins, such as the DNA polymerase POLB. To identify potential candidates for peroxisomal targeting, we examined multiple alignments with orthologous proteins from other plants (see Methods for details) in search of the same conservation scheme observed in TTL: high conservation at positions +1, +2, +5, +8, and +9 and low conservation at positions −1, +3, +4, +6, +7, and +10. Through this analysis we rediscovered the internal signal of TTL and found several other proteins with N-terminal PTS2s but no other candidates for internal PTS2s.

METHODS

Cloning, Gene Expression, and Protein Purification

TTL transcripts were amplified from cDNA generated from total RNA extracted from *Arabidopsis thaliana* seedlings using primers 5′-ttcggtccgATGGCGATGGAGATCGGAG-3′ and 5′-ttcggaccgCTAGCTCCCACGGTATGTGGAGAAAG-3′. All the primers bore 5′-tails such that the amplification products contained *Cpo*I target sequences near to both ends. Amplicons were cloned into pGEM T-Easy vector (Promega). Plasmids were then inserted into XL1B *Escherichia coli* cells (Stratagene) and the inserts were sequence verified. The plasmids were subsequently treated with *Cpo*I to extract the fragments corresponding to the amplified full-length coding sequence, ready for subcloning into the expression vector pET28-CpoI. This plasmid is a derivative of pET28 (Novagen) modified to present a single *Cpo*I restriction site in the cloning region, downstream to a sequence encoding a hexa-histidine tag (A. Bolchi, unpublished data). *E. coli* BL21 (DE3) codon plus cells (Stratagene) transformed with TTL^{1-}-pET28-CpoI or TTL^{2-}-pET28-CpoI constructs were incubated at 37°C in a M9 minimal medium until they reached the optical density of 0.6 at 600 nm. Expression was induced by adding 1 mM

isopropyl β-D-1-thiogalactopyranoside (IPTG) and transferring the culture to 4°C for 3 d.

Cells from 250 mL of culture were lysed by 60 30-min bursts of sonication in 100 mL of 50 mM sodium phosphate, 300 mM NaCl, 10% glycerol, and 0.005% Tween 20, pH 7.5. Proteins were purified by TALON metal affinity resin (Clontech) and eluted by adding 100 mM imidazole with a final yield of ~4 mg per liter of cell culture.

Biochemical Assays

The enzymatic activity of TTL^1 TTL^2 splice variants was monitored by CD measurements performed in a 10-mm pathlength cuvette with a Jasco J715 spectropolarimeter. The degradation of urate (0.1 mM) in 1 mL of 0.1 M potassium phosphate, pH 7.6, was monitored in the 200- to 350-nm range in the presence of urate oxidase from *Candida utiliz* (0.8 units; Sigma-Aldrich) and in the presence or in absence of TTL^1 or TTL^2. Single length measurements were performed for HIUase activity at 312 nm and for OHCU decarboxylase activity at 257 nm in presence of 0.6 μg of zebrafish HIUase (Zanotti et al., 2006). Activities of the bifunctional TTL protein were compared with the activities of zebrafish HIUase and OHCU decarboxylase (Cendron et al., 2007) monitored by single length measurements in the same reaction conditions.

Plant Material and Growth Conditions

Standard *Arabidopsis* ecotype Columbia-0 was obtained from the European Arabidopsis Stock Centre. *Oryza sativa* (Vialone nano, japonica) was obtained from CRA-GPG (Fiorenzuola d'Arda). Seed sterilization, germination, and plate culture of seedlings were performed following the protocols recommended by the ABRC. Plants were grown in a greenhouse in 16-h-light/8-h-dark cycle at 25°C. Protoplast isolation (Abel and Theologis, 1994) was conducted on plants grown 3 to 4 weeks in soil. Total RNA was isolated from plants grown 4 weeks in soil (plant tissues) or from plants grown 3 d on plates with Murashige and Skoog (MS) medium (total seedlings). Growth on different nitrogen sources was conducted on MS medium without nitrogen, supplemented with 5 mM urate, 5 mM urate plus 5 mM NH_4NO_3, or 5 mM allantoin. Urate was dissolved in MS medium at ~50°C. Precipitation of urate was apparent after solidification of agar plates; however, a clear area was observed around the plant roots. For dark treatment, 4-week-old plants grown on soil were transferred to a dark room. Rosette leaves were collected after 2, 4, and 6 d of dark treatment.

In Vivo Targeting of Fusion Proteins

To generate the chimeric fusion constructs, TTL^1-pET28Cpol and TTL^2-pET28Cpol were used as templates for amplification with PfuUltra polymerase (Stratagene) using primers At5g58220for, 5′-taggatccaaaaATGGCGATGGAGATCGGA-3′, and At5g58220rev, 5′-tgctcaccatGCTCCCACGGTATGTGGA-3′, introducing a *Bam*HI site plus a plant ribosome binding site at the 5′-end and a GFP sequence (10 nucleotides) at the 3′-end. Primer At5g58220rev eliminates the TAA stop codon from TTL^1 and TTL^2, allowing GFP fusion. GFP was amplified using primers GFPfor, 5′-taccgtgggagcATGGTGAGCAAGGGCGAG- 3′, and GFPrev, 5′-ttgagctcTTACTTGTACAGCTCGTCC-3′, introducing a TTL sequence (12 nucleotides) at the 5′-end of GFP and a 3′ *Sac*I site. A third PCR with primers At5g58220for and GFPrev, using as templates GFP and TTL^1 or TTL^2 gave the fusion constructs TTL^1-GFP and TTL^2 -GFP, which were cloned in pNEB193 following published protocols (Bolchi et al., 2005). The ligated plasmids were then transformed into XL1B *E. coli* cells (Stratagene) and the inserts were sequence verified. The plasmids were subsequently treated with *Bam*HI and *Sac*I and subcloned into the plant expression vector pPZPY122 (Yamamoto et al., 1998).

The YFP-SKL peroxisome marker was amplified by PCR with primers 5′-ttggtaccaaaaATGGTGAGCAAGGGCGAG-3′, and 5′-ttctagatttacaattttgaCTTGTACAGCTCGTCC-3′, introducing a *Bam*HI site plus a plant ribosome binding site at the 5′-end and a PTS1 sequence plus a *Kpn*I site at the 3′-end. The YFP cytoplasm marker was amplified with primers 5′-ttggtaccaaaaATGGTGAGCAAGGGCGAG-3′ and 5′-attctagaTTACTTGTACAGCTCGTCCATG-3′, introducing a *Bam*HI site plus a plant ribosome binding site at the 5′-end and a *Xba*I site at the 3′-end. YFP and YFP-SKL were cloned in pART7 vector following published protocols (Bolchi et al., 2005) and the inserts were sequence verified.

The fusion constructs were introduced by polyethylene glycol–mediated transformation into *Arabidopsis* protoplasts prepared from plant leaves (Abel and Theologis, 1994). Transformed protoplasts were incubated in darkness at 23°C for 16 to 24 h before checking the fluorescence. Cells were mounted in custom-made chambers (Gatti et al., 2008) and observed by confocal microscopy (×100 objective lens, 488-nm excitation) using a LSM 510 Meta scan head equipped with an Axiovert 200 M inverted microscope (Carl Zeiss).

RNA Isolation and RT-PCR

Tissues for total RNA preparation were frozen in liquid nitrogen and pulverized using a pestle. The powdered tissues were transferred in a buffer containing 0.6 M NaCl, 4% SDS, 10 mM EDTA, and 100 mM Tris-HCl, pH 8. Total RNA was isolated following a described miniprep procedure (Sokolowsky et al., 1990) except that phenol:chloroform (1:1) was used for extraction. RNA was recovered by precipitation in 4.4 M LiCl. Reverse transcription of 2 μg of total RNA was performed with Superscript III reverse transcriptase (Invitrogen) and an oligo(dT) primer in a 20-μL reaction. A 2-μL aliquot of the reaction mixture was used as a template for PCR amplification with TTL-specific primers designed to discriminate TTL^1 and TTL^2 transcripts in *Arabidopsis* (forward primer, 5′-GCTCTCCTGTTTCAACAAAACC- 3′; reverse primer, 5′-GGATTCAAAGCGTCAACCAAATC-3′) and *O. sativa* (forward primer, 5′-AGAACTGAAGATAACTGAACTGCG-3′; reverse primer, 5′-GGTGTTGATGCATCCTTCCACAT-3′). Reactions conducted on RNA extracted from different plant tissues were normalized with the Elongation factor 1α (At5g60390) as housekeeping gene (forward primer, 5′-GGCTGATTGTCAGACCCGTGAGCAC-3′; reverse primer, 5′-GGAGTATTTGGGGGTGGTGGCATCCAT-3′). The senescence-related gene 1 (At1g17020) was used as a reference dark-induced gene (forward primer, 5′-AAGAGTGGGGATTTTTCCAGCTTGT-3′; reverse primer, 5′-TGCCCAATCTAGTTTCTGATCTTCTGA-3′). Twenty and thirty PCR cycles were used to amplify reference transcripts and TTL transcripts, respectively. Reactions conducted at a different number of cycles showed that the ratio between TTL^1 and TTL^2 forms was not altered by PCR saturation, indicating the existence of a Ratio PCR condition (Raeymaekers, 1995). PCR products were loaded on agarose 1.8% TBE gel, stained with ethidium bromide, and analyzed with the Multi-Analyst/PC software (Bio-Rad).

Bioinformatics

Sequence alignments were performed with ClustalW (Thompson et al., 1994) and visualized with Espript (Gouet et al., 1999). Comparisons of alternative transcript sequences with genomic sequences were performed with Genewise (Birney et al., 2004). In silico identification of TTL splice variants in plant sequences was performed using the TIGR plant transcript assemblies database (http://plantta.jcvi.org/) using the *Arabidopsis* protein sequence and the tBLASTn program. Search of PTS2 sequence pattern was performed with the Fuzzpro program of the EMBOSS package (http://emboss.sourceforge.net) using the complete set of *Arabidopsis* proteins downloaded from the National Center for Biotechnology Information ftp site (ftp://ftp.ncbi.nih.gov). Conservation of putative PTS2 sequences in orthologous proteins from other plants was examined to identify spurious occurrence of the motif. Orthology was assessed by applying the Best Reciprocal Hit method to BLAST

homology searches conducted against complete sets of protein sequences from *Chlamydomonas reinhardtii*, *Physcomitrella patens*, *Vitis vinifera*, *Populus trichocarpa*, and *O. sativa*. Phylogenetic analysis was performed on the separated Urah and Urad domains using the protein maximum likelihood method implemented in the Proml program of PHYLIP (http://evolution.genetics.washington.edu). Trees were rooted by midpoint using the Retree program of PHYLIP and visualized with Treeillustrator (http://nexus.ugent.be/geert).

Accession Numbers

Sequence data determined for TTL^1 and TTL^2 cDNAs have been submitted to GenBank under accession numbers GQ303357 (TTL^1) and GQ303358 (TTL^2). Accession numbers of the sequences used for multiple alignment and phylogenetic reconstruction are listed in Supplemental Table 1 online.

Supplemental Data

The following materials are available in the online version of this article.

Supplemental Figure 1. TTL Expression and Affinity Column Purification.

Supplemental Figure 2. In Vivo Localization of GFP-TTL^1 Fusion Protein.

Supplemental Figure 3. Alternative Splicing in *Oryza sativa* TTL.

Supplemental Figure 4. RT-PCR Analysis of TTL Splice Variants in the Presence of Different Nitrogen Sources.

Supplemental Figure 5. RT-PCR Analysis of TTL Splice Variants in Dark-Treated Plants.

Supplemental Figure 6. Molecular Phylogeny of the *urad-urah* Gene Fusion in Plants and Bacteria.

Supplemental Table 1. Database Accession Numbers of the Sequences Used in This Study.

Supplemental Data Set 1. Text File of uraH Domain Alignment Corresponding to Supplemental Figure 6.

Supplemental Data Set 2. Text File of uraD Domain Alignment Corresponding to Supplemental Figure 6.

ACKNOWLEDGMENTS

We thank Francesco Restivo, Luigi Cattivelli, and Caterina Marè for the kind gift of materials, Ileana Ramazzina for help with CD measurements, Angelo Bolchi, Anna Torelli, Barbara Montanini, Davide Martorana, and Roberto Viscomi for their assistance, and Alessio Peracchi for discussions. We had the privilege of sharing research and personal thoughts with the senior author. We will always cherish memories of her.

Received July 15, 2009; revised April 14, 2010; accepted May 10, 2010; published May 28, 2010.

REFERENCES

Abel, S., and Theologis, A. (1994). Transient transformation of Arabidopsis leaf protoplasts: A versatile experimental system to study gene expression. Plant J. **5:** 421–427.

Barbazuk, W.B., Fu, Y., and McGinnis, K.M. (2008). Genome-wide analyses of alternative splicing in plants: Opportunities and challenges. Genome Res. **18:** 1381–1392.

Birney, E., Clamp, M., and Durbin, R. (2004). GeneWise and Genomewise. Genome Res. **14:** 988–995.

Bolchi, A., Ottonello, S., and Petrucco, S. (2005). A general one-step method for the cloning of PCR products. Biotechnol. Appl. Biochem. **42:** 205–209.

Brychkova, G., Alikulov, Z., Fluhr, R., and Sagi, M. (2008). A critical role for ureides in dark and senescence-induced purine remobilization is unmasked in the Atxdh1 Arabidopsis mutant. Plant J. **54:** 496–509.

Cendron, L., Berni, R., Folli, C., Ramazzina, I., Percudani, R., and Zanotti, G. (2007). The structure of 2-oxo-4-hydroxy-4-carboxy-5-ureidoimidazoline decarboxylase provides insights into the mechanism of uric acid degradation. J. Biol. Chem. **282:** 18182–18189.

de la Fuente van Bentem, S., Vossen, J.H., Vermeer, J.E., de Vroomen, M.J., Gadella, T.W., Jr., Haring, M.A., and Cornelissen, B.J. (2003). The subcellular localization of plant protein phosphatase 5 isoforms is determined by alternative splicing. Plant Physiol. **133:** 702–712.

Desimone, M., Catoni, E., Ludewig, U., Hilpert, M., Schneider, A., Kunze, R., Tegeder, M., Frommer, W.B., and Schumacher, K. (2002). A novel superfamily of transporters for allantoin and other oxo derivatives of nitrogen heterocyclic compounds in *Arabidopsis*. Plant Cell **14:** 847–856.

Dixon, D.P., Hawkins, T., Hussey, P.J., and Edwards, R. (2009). Enzyme activities and subcellular localization of members of the Arabidopsis glutathione transferase superfamily. J. Exp. Bot. **60:** 1207–1218.

Eubel, H., Meyer, E.H., Taylor, N.L., Bussell, J.D., O'Toole, N., Heazlewood, J.L., Castleden, I., Small, I.D., Smith, S.M., and Millar, A.H. (2008). Novel proteins, putative membrane transporters, and an integrated metabolic network are revealed by quantitative proteomic analysis of Arabidopsis cell culture peroxisomes. Plant Physiol. **148:** 1809–1829.

Gatti, R., Orlandini, G., Uggeri, J., Belletti, S., Galli, C., Raspanti, M., Scandroglio, R., and Guizzardi, S. (2008). Analysis of living cells grown on different titanium surfaces by time-lapse confocal microscopy. Micron **39:** 137–143.

Gouet, P., Courcelle, E., Stuart, D.I., and Metoz, F. (1999). ESPript: Analysis of multiple sequence alignments in PostScript. Bioinformatics **15:** 305–308.

Hanks, J.F., Tolbert, N.E., and Schubert, K.R. (1981). Localization of enzymes of ureide biosynthesis in peroxisomes and microsomes of nodules. Plant Physiol. **68:** 65–69.

Hayashi, M., Tsugeki, R., Kondo, M., Mori, H., and Nishimura, M. (1996). Pumpkin hydroxypyruvate reductases with and without a putative C-terminal signal for targeting to microbodies may be produced by alternative splicing. Plant Mol. Biol. **30:** 183–189.

Helm, M., Luck, C., Prestele, J., Hierl, G., Huesgen, P.F., Frohlich, T., Arnold, G.J., Adamska, I., Gorg, A., Lottspeich, F., and Gietl, C. (2007). Dual specificities of the glyoxysomal/peroxisomal processing protease Deg15 in higher plants. Proc. Natl. Acad. Sci. USA **104:** 11501–11506.

Hennebry, S.C., Wright, H.M., Likic, V.A., and Richardson, S.J. (2006). Structural and functional evolution of transthyretin and transthyretin-like proteins. Proteins **64:** 1024–1045.

Jung, D.K., Lee, Y., Park, S.G., Park, B.C., Kim, G.H., and Rhee, S. (2006). Structural and functional analysis of PucM, a hydrolase in the ureide pathway and a member of the transthyretin-related protein family. Proc. Natl. Acad. Sci. USA **103:** 9790–9795.

Kahn, K., and Tipton, P.A. (1998). Spectroscopic characterization of intermediates in the urate oxidase reaction. Biochemistry **37:** 11651–11659.

Kazan, K. (2003). Alternative splicing and proteome diversity in plants: The tip of the iceberg has just emerged. Trends Plant Sci. **8:** 468–471.

Kiel, J.A., van den Berg, M.A., Fusetti, F., Poolman, B., Bovenberg, R.A., Veenhuis, M., and van der Klei, I.J. (2009). Matching the proteome to the genome: The microbody of penicillin-producing *Penicillium chrysogenum* cells. Funct. Integr. Genomics **9:** 167–184.

Kim, K., Park, J., and Rhee, S. (2007). Structural and functional basis for (S)-allantoin formation in the ureide pathway. J. Biol. Chem. **282:** 23457–23464.

Miles, E.W., Rhee, S., and Davies, D.R. (1999). The molecular basis of substrate channeling. J. Biol. Chem. **274:** 12193–12196.

Nam, K.H., and Li, J. (2004). The *Arabidopsis* transthyretin-like protein is a potential substrate of BRASSINOSTEROID-INSENSITIVE 1. Plant Cell **16:** 2406–2417.

Prassinos, C., Haralampidis, K., Milioni, D., Samakovli, D., Krambis, K., and Hatzopoulos, P. (2008). Complexity of Hsp90 in organelle targeting. Plant Mol. Biol. **67:** 323–334.

Puyaubert, J., Denis, L., and Alban, C. (2008). Dual targeting of Arabidopsis holocarboxylase synthetase1: A small upstream open reading frame regulates translation initiation and protein targeting. Plant Physiol. **146:** 478–491.

Raeymaekers, L. (1995). A commentary on the practical applications of competitive PCR. Genome Res. **5:** 91–94.

Ramazzina, I., Folli, C., Secchi, A., Berni, R., and Percudani, R. (2006). Completing the uric acid degradation pathway through phylogenetic comparison of whole genomes. Nat. Chem. Biol. **2:** 144–148.

Raychaudhuri, A., and Tipton, P.A. (2002). Cloning and expression of the gene for soybean hydroxyisourate hydrolase. Localization and implications for function and mechanism. Plant Physiol. **130:** 2061–2068.

Reddy, A.S. (2007). Alternative splicing of pre-messenger RNAs in plants in the genomic era. Annu. Rev. Plant Biol. **58:** 267–294.

Reumann, S., Babujee, L., Ma, C., Wienkoop, S., Siemsen, T., Antonicelli, G.E., Rasche, N., Luder, F., Weckwerth, W., and Jahn, O. (2007). Proteome analysis of *Arabidopsis* leaf peroxisomes reveals novel targeting peptides, metabolic pathways, and defense mechanisms. Plant Cell **19:** 3170–3193.

Sammeth, M., Foissac, S., and Guigo, R. (2008). A general definition and nomenclature for alternative splicing events. PLOS Comput. Biol. **4:** e1000147.

Schubert, K.R. (1986). Products of biological nitrogen fixation in higher plants: Synthesis, transport, and metabolism. Annu. Rev. Plant Physiol **37:** 539–573.

Sokolowsky, V., Kaldenhoff, R., Ricci, M., and Russo, V. (1990). Fast and reliable mini-prep RNA extraction from *Neurospora crassa*. Fungal Genet. Newsl. **37:** 41–43.

Thompson, J.D., Higgins, D.G., and Gibson, T.J. (1994). CLUSTAL W: Improving the sensitivity of progressive multiple sequence alignment through sequence weighting, position-specific gap penalties and weight matrix choice. Nucleic Acids Res. **22:** 4673–4680.

Todd, C.D., Tipton, P.A., Blevins, D.G., Piedras, P., Pineda, M., and Polacco, J.C. (2006). Update on ureide degradation in legumes. J. Exp. Bot. **57:** 5–12.

Wang, B.B., and Brendel, V. (2006). Genomewide comparative analysis of alternative splicing in plants. Proc. Natl. Acad. Sci. USA **103:** 7175–7180.

Werner, A.K., Sparkes, I.A., Romeis, T., and Witte, C.P. (2008). Identification, biochemical characterization, and subcellular localization of allantoate amidohydrolases from Arabidopsis and soybean. Plant Physiol. **146:** 418–430.

Worden, A.Z., et al. (2009). Green evolution and dynamic adaptations revealed by genomes of the marine picoeukaryotes Micromonas. Science **324:** 268–272.

Yamamoto, Y.Y., Matsui, M., Ang, L.H., and Deng, X.W. (1998). Role of a COP1 interactive protein in mediating light-regulated gene expression in *Arabidopsis*. Plant Cell **10:** 1083–1094.

Zanotti, G., Cendron, L., Ramazzina, I., Folli, C., Percudani, R., and Berni, R. (2006). Structure of zebra fish HIUase: Insights into evolution of an enzyme to a hormone transporter. J. Mol. Biol. **363:** 1–9.